small NANO MICRO

Nanoparticle Sheets

In-Situ Partial Sintering of Gold-Nanoparticle Sheets for SERS Applications

*Jinbo He, Xiao-Min Lin, Ralu Divan, and Heinrich M. Jaeger**

***A** new, versatile substrate design for surface-enhanced Raman spectroscopy (SERS) is introduced that provides better illumination and collection efficiency than other solid substrates. It uses sheets of 5 nm diameter gold nanoparticles that are draped by drying-mediated self-assembly onto 100 nm thick silicon nitride membranes. During laser illumination, partial in-situ sintering of the nanoparticles into larger structures with tiny gaps (≈2 nm) greatly increases the SERS enhancement factor. The detection of 1 pM of p-mercaptoaniline and 1 fg of 2,4-dinitrotoluene is demonstrated. The use of self-assembled nanoparticle sheets furthermore makes it possible to perform SERS detection in situ on top of a probe solution droplet.*

1. Introduction

Ever since the discovery of surface-enhanced Raman spectroscopy (SERS), the technique has generated tremendous interest due to its ultrahigh sensitivity, with potential applications in chemical and biological sensors.[1] Different approaches for fabricating SERS substrates using "top-down" or "bottom-up" methods, or a combination of both, have been studied extensively.[2] SERS substrates based on colloidal metal nanoparticles have received special attention because of the possibility to reach enhancement factors as large as 10^{14}–10^{15} from a combination of electromagnetic and chemical enhancement effects, which has brought single-molecule detection within reach.[3] To achieve such enormous enhancement, nanostructures of suitable size and separation distances (less than a few nanometers) are crucial.[4] In previous studies, this was achieved by inducing the aggregation of nanocrystals in a solvent, while they were incubated with the probe molecules.[3] This approach produces good results in terms of illumination and the likelihood of embedding probing molecules into "hot spots", but these advantages are lost when the nanoparticles are dried onto a substrate.[5]

The fabrication of a high-sensitivity SERS substrate has remained a challenge, mainly because of the difficulty in producing the optimal configuration of metal particles a few tens of nanometers in size and at the same time separated by gaps of only a few nanometers. In this regard, self-assembly of ligated metal nanoparticles offers much potential,[5c,6] and in hexagonally packed arrays enhancement factors up to 10^8 have been reported.[6a,c] However, the assembly of large, 10–30-nm-diameter metal nanoparticles into ordered arrays requires engineering of a thick ligand coating to balance the strong van der Waals attraction between neighboring metal cores and prevent sintering. In practice, this leads to fairly large (8–10 nm) ligand-filled gaps between nanoparticles, and the dense ligand packing also presents a barrier for probe molecules to diffuse into interstitial "hot spots".[5c,7]

Herein, we report a simple alternative approach to self-assemble highly sensitive SERS substrates that circumvent some of these problems, can reach enhancement factors $>10^9$, and can be used for the detection of molecules in the liquid, solid, and possibly gas phases. Our key idea is to utilize the highly controllable, drying-mediated self-assembly of small (≈5.5 nm in diameter) metal nanoparticles to form close-packed monolayer sheets with 1–2 nm interparticle gaps. Laser illumination for the SERS measurement provides the particles with sufficient mobility to enable partial, in-situ sintering into 10–50 nm structures that remain surrounded by closely spaced neighbors. We also demonstrate that the type of solid support for the nanoparticles can have a significant influence on the observed SERS signal. In contrast to the usual

Dr. J. He, Prof. H. M. Jaeger
James Franck Institute
The University of Chicago
Chicago, IL 60637, USA
E-mail: h-jaeger@uchicago.edu
Dr. X.-M. Lin, Dr. R. Divan
Center for Nanoscale Materials
Argonne National Laboratory
Argonne, IL 60439, USA

DOI: 10.1002/smll.201101534

© 2011 Wiley-VCH Verlag GmbH & Co. KGaA, Weinheim

thick solid support, a 100 nm thin silicon nitride membrane is shown to allow for total internal reflection of the excitation laser beam and to maximize the local excitation field, which induces additional enhancement of the SERS signal.

2. Results and Discussion

Figure 1a illustrates the main features of our SERS substrate. It consists of a 3 mm × 4 mm piece of silicon wafer coated with Si_3N_4 and back-etched over a 60 μm × 60 μm square area to create 100 nm thin "window" membranes. Dodecanethiol-stabilized gold nanocrystals with core sizes ≈5.5 nm (<10% size within each batch) were synthesized by the digestive ripening protocol, as described earlier.[8] A nanoparticle monolayer was formed by a one-step drying method that self-assembles nanoparticles at the liquid/air interface of a water droplet deposited on the substrate. The monolayer then draped itself over the substrate once the water evaporated.[7a,9] Figure 1b shows an optical microscopy image of a sample partially covered by a layer of gold nanoparticles. The thicker regions are the result of folds in the monolayer sheet, formed during the drying and draping process. The well-ordered, close-packed structure of a single layer is demonstrated by the transmission electron microscopy (TEM) image shown in Figure 1c, taken in the window area.

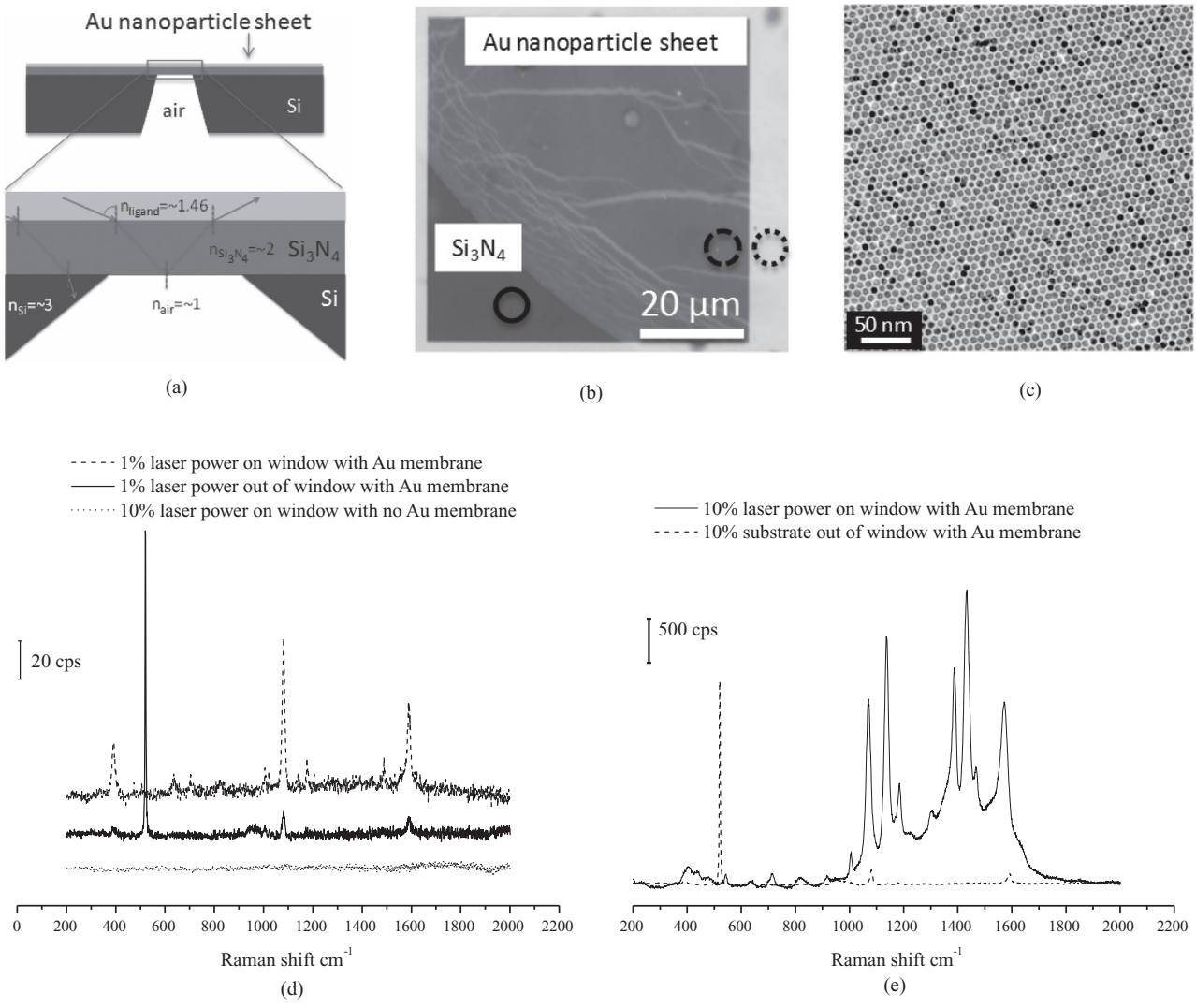

Figure 1. a) Schematic cross section of the SERS substrate: 3 mm × 4 mm silicon coated with a 100-nm-thick silicon nitride film. The silicon was etched away from the back side to create square, 60 μm × 60 μm silicon nitride "window" areas. Gold-nanoparticle sheets were draped over the substrate by using a drying-mediated self-assembly process. The zoomed-in view sketches the reflected and refracted light paths. b) Optical microscopy image (top view) of a Si_3N_4 window area partially covered with a gold-nanoparticle sheet. c) TEM image of a dried nanoparticle sheet in the window area, prior to laser illumination. d) Raman spectra collected both inside (dashed line) and outside the window area (solid line) at 1% laser power (47 μW), after 1 mM *p*MA (8 μL) was dried on the substrate. As a baseline, the black trace shows the signal at 10% laser power taken at a bare spot inside the window without gold nanoparticles. The circles in (b) represent the positions where Raman spectra were collected. e) Same as (d) but with 10% laser power (0.47 mW), comparing the SERS signals from nanoparticle sheets inside (solid line) and outside the window area (dashed line). For both (d) and (e) the excitation wavelength was 633 nm and the acquisition time was 10 s per trace.

© 2011 Wiley-VCH Verlag GmbH & Co. KGaA, Weinheim

small NANO MICRO

To test the sensitivity of the SERS substrate, we deposited 1 mM *p*-mercaptoaniline (*p*MA; 8 μL) solution on top of the chip and let it dry under ambient conditions. SERS spectra were obtained with a Renishaw inVisa Raman microscope using a 50× objective with numerical aperture (NA) 0.75. A He–Ne laser with wavelength 633 nm and power 4.7 mW at 100% was used for excitation. The laser beam focused on the samples was ≈2 μm in diameter.

In a first set of baseline measurements, we probed the surface with 1% laser power (47 μW). With such low laser power, there is no rearrangement or damage to the nanoparticle assembly, as confirmed by TEM. Figure 1d shows the SERS spectra taken at different positions marked in the optical image in Figure 1b. In the area just outside the Si_3N_4 windows, weak SERS signals of *p*MA were detected (solid curve in Figure 1d). Two characteristic Raman peaks at 1080 and 1590 cm^{-1} can be attributed to the vibrational modes of *p*MA exhibiting *a*1 symmetry with respect to the C_{2v} symmetry group of the molecule.[2d,10] No strong modes of *b* symmetry are observed. The low enhancement of the SERS signal is in line with the small size of the gold cores, as predicted by theoretical studies.[4] However, on the Si_3N_4 windows, the SERS signal at 1% laser power (dashed curve in Figure 1d) is enhanced by at least one order of magnitude as compared with signals from outside the window area. Statistical sampling confirmed that this is not caused by heterogeneous distribution of the probe molecules.

This extra enhancement on the window is due to the design of the substrate, which can effectively reflect the incident light and Raman scattering at the Si_3N_4/air interface, as illustrated in Figure 1a. Since the refractive indices of ligand, Si_3N_4, Si, and air are 1.46, 2, 3, and 1, respectively, light at high incident angle is expected by Snell's law to exhibit total internal reflection at the Si_3N_4/air interface, but not at the Si_3N_4/Si interface. Indeed, with the type of large-NA objective lens normally used in Raman spectroscopy to collect more signal,[11] laser beams with incident angle >43° in the gold-nanoparticle sheet (>30° in the Si_3N_4 layer) did show total reflection at the Si_3N_4/air interface. But the majority of the incident beam will be partially reflected. This partially reflected beam, on the one hand, provides better illumination compared to previous approaches using thick solid substrates. On the other hand, interference between multiply reflected beams may also contribute to the Raman enhancement factor as previously reported.[12] Furthermore, Raman scattering is angle dependent with a maximum intensity at 55–60° away from the surface normal.[6a,13] Wei and co-workers have demonstrated that, by increasing the NA from 0.25 to 0.75, the enhancement factor was increased by an order of magnitude. This high-angle, high-intensity Raman signal would have been lost in other solid substrates. But because of the total reflection at the Si_3N_4/air interface, it was collected by the objective lens in our experiment. Finally, further enhancement of the SERS signal can in principle arise from multiple internal reflections and passage of the scattered Raman signal through "hot spots".

When we increased the laser to 10% of its full power (i.e., to 0.47 mW) and probed the area outside the Si_3N_4 window, the SERS signals at 1080 and 1590 cm^{-1} increased by about the same order of magnitude as the incident beam (dashed curve, Figure 1e). However, inside the Si_3N_4 window area covered with gold nanoparticles, a huge enhancement was found and the peak features changed, as indicated by the black curve in Figure 1e. Importantly, three additional, strongly enhanced peaks at 1136, 1387, and 1433 cm^{-1} are observed, which can be uniquely assigned to the mode with *b*2 symmetry.[2d,10] The appearance of *b*2 modes with increasing laser power has previously been observed in Au-nanoparticle aggregates and was attributed to the quinonoid form of *p*MA molecules bridging neighboring nanoparticles.[14] Charge transfer between the *p*MA molecules and the metal surfaces is largely believed to cause the tautomerization of benzenoid and quinonoid states of *p*MA molecules.[2d,10] However, Wu et al. have recently proposed that *p*,*p*′-dimercaptoazobenzene created by surface catalytic reactions is responsible for the *b*2 mode.[15]

Regardless of the detailed mechanism, the *b*2 mode of *p*MA molecules is a signature of chemical enhancement effects that require these molecules to be in direct contact with a metal surface.[2d,10] The presence of these three strong peaks in the Si_3N_4 window area therefore indicates a structural change of the nanoparticle assembly, which allows the probe molecules to get closer to the gold cores so that chemical enhancement can take place.

A TEM image of a nanoparticle layer in the window area after being exposed to 10% laser power is shown in **Figure 2**a. We find partial sintering of the gold nanoparticles, presumably due to the lack of efficient heat dissipation at the window area. Chains of smaller particles (10–20 nm in diameter, sintered in the monolayer regions) and larger nanoparticles (40–50 nm in diameter, sintered in regions of multilayers due to folds) with ≈2 nm gaps are seen, as well as "satellite" structures of larger nanoparticles surrounded by several smaller nanoparticles. These structures are generally present at the samples with the same experimental conditions (as shown in Figure S1a,b, Supporting Information), which indicates a good reproducibility of the current setup. We note that outside of the window area, as shown in Figure S1c,d, no damage to the gold-nanoparticle sheets at 10% laser power is visible by scanning electron microscopy (SEM). Such structures and combinations of particle sizes are known to be favorable for strong SERS enhancement.[5b,16] The sintering of gold nanoparticles into nanowire networks at water/air interfaces has been reported previously.[17] However, in that work particles were found to coalesce and well-defined nanoscale gaps were absent, which limits the SERS enhancement.[4]

Using small nanoparticles as a precursor, the in-situ sintering provides both the "hot spots" and more opportunities for probe molecules to get into them, without requiring sophisticated synthesis procedures or lithography to form specific nanoparticle arrangements.[18] Results also indicated that with the current setup, the method also provides high reproducibility since the wrinkles are generally everywhere. Indeed, our method can detect extremely low concentrations of the probe molecule *p*MA. As we decrease the concentration of *p*MA in solution down to 1 pM, the characteristic SERS peaks can still be identified (Figure 2b). To calculate the empirical enhancement factor we compared the ratio of the physically enhanced 1080 cm^{-1} SERS peak intensity to the corresponding unenhanced signal from neat *p*MA films of known thickness on the Si_3N_4 window (see the Supporting

 © 2011 Wiley-VCH Verlag GmbH & Co. KGaA, Weinheim

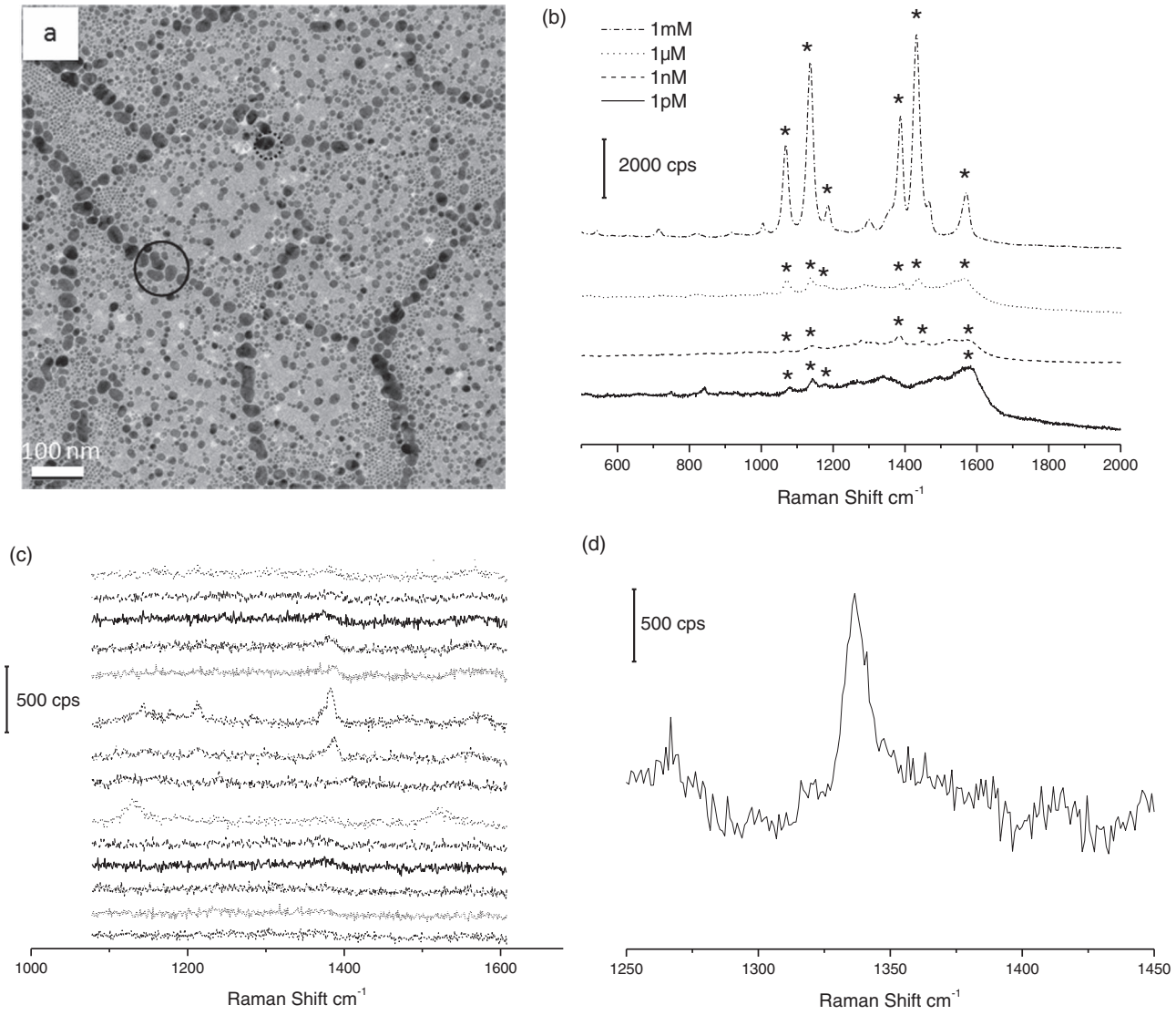

Figure 2. a) TEM image of a spot inside the Si_3N_4 window area that was exposed to 10% laser power for 10 s. Partial annealing by the laser illumination produced assemblies of large nanoparticles with very narrow gaps (the solid circle indicates an example), as well as "satellite" structures (dashed circle). b) SERS spectra of *p*MA at different concentrations. Stars indicate characteristic Raman peaks of *p*MA. The curves are moved vertically for clarity. Excitation wavelength: 633 nm; laser power: 10% (0.47 mW); acquisition time: 10 s. c) Fast-scan SERS spectra of *p*MA at 1 pM. Curves are shifted vertically for clarity. Excitation wavelength: 633 nm; laser power: 10% (0.47 mW); acquisition time: 1 s per trace. d) SERS spectrum of 2,4-DNT (5 μL, 1 μg mL^{-1}) acetonitrile solution deposited onto the chip. The NO_2 stretching mode at 1334 cm^{-1} is clearly seen. Excitation wavelength: 633 nm; laser power: 1% (47 μW); acquisition time: 10 s.

Information for details). From the 1 pM data, a conservative empirical enhancement factor of $\approx 4 \times 10^9$ is estimated. At 1 pM concentration, only a few *p*MA molecules are present within the area illuminated by the laser, assuming a homogeneous distribution of molecules on the substrate. Being able to detect *p*MA molecules under such conditions indicates that the local enhancement factor inside the interparticle interstices is significantly larger than 4×10^9.

To check if this allows us to detect the signature of individual molecules we looked for blinking, a phenomenon in which the SERS signal goes on and off due to the diffusion of probe molecules into and out of hot spots.[1d,3a,b] This blinking behavior is indeed observed at very low concentrations of *p*MA, but is much slower than that found in experiments using colloids in solution, presumably due to the very low diffusion rate in our dried solid film. Figure 2c shows a subset from 60 continuous SERS scans, all taken at a fixed position with 1 s exposure time each (see Figure S3 for all 60 scans). At the beginning (bottom trace), only the flat background is observed. At certain points later in time, strong SERS signals associated with several of the characteristic peak positions appear and then disappear (Figure 2b), an indication that molecules diffuse into hot spots, explore different orientations, and produce a time-varying chemically enhanced Raman signal. While not a direct proof, this nevertheless indicates that our SERS substrate may have the ability to detect single molecules.

This high sensitivity opens up opportunities for the detection of molecules associated with common explosives. To demonstrate this capability, we used 2,4-dinitrotoluene (2,4-DNT). A 2,4-DNT acetonitrile solution (5 μL, 1 μg mL^{-1})

© 2011 Wiley-VCH Verlag GmbH & Co. KGaA, Weinheim

small NANO MICRO

was dried onto the substrate and the resulting SERS spectrum is shown in Figure 2d. The key vibration mode for 2,4-DNT, the NO_2 stretching mode at 1334 cm^{-1}, is clearly observed, consistent with previous reports.[19] Considering the total amount (5 ng) of 2,4-DNT spread over the whole 3 mm × 4 mm area and assuming a homogeneous distribution, we achieved a sensitivity of ≈1 fg with our 2-μm-diameter laser beam spot. This pushes the detection limit three orders of magnitude lower than previously reported.[19]

Finally, using our preparation method, the nanoparticles form a compact sheet while still at the air/water interface, long before the water droplet has evaporated, and the sheet drapes itself over the solid substrate.[7a,9] This makes it possible to use our approach for in-situ SERS detection, that is, deposition of a SERS-active nanoparticle array directly on top of a water droplet containing probe molecules. **Figure 3**a shows an optical image of the gold-nanoparticle membrane on top of a water droplet containing *p*MA molecules. Figure 3b shows SERS spectra for different *p*MA concentrations, taken in situ by focusing on the top of the water droplet, as illustrated in the inset to Figure 3a. In this case, the silicon nitride window substrate does not contribute additional enhancement, but the characteristic Raman peaks of *p*MA in solutions as dilute as 1 nM can still be identified.

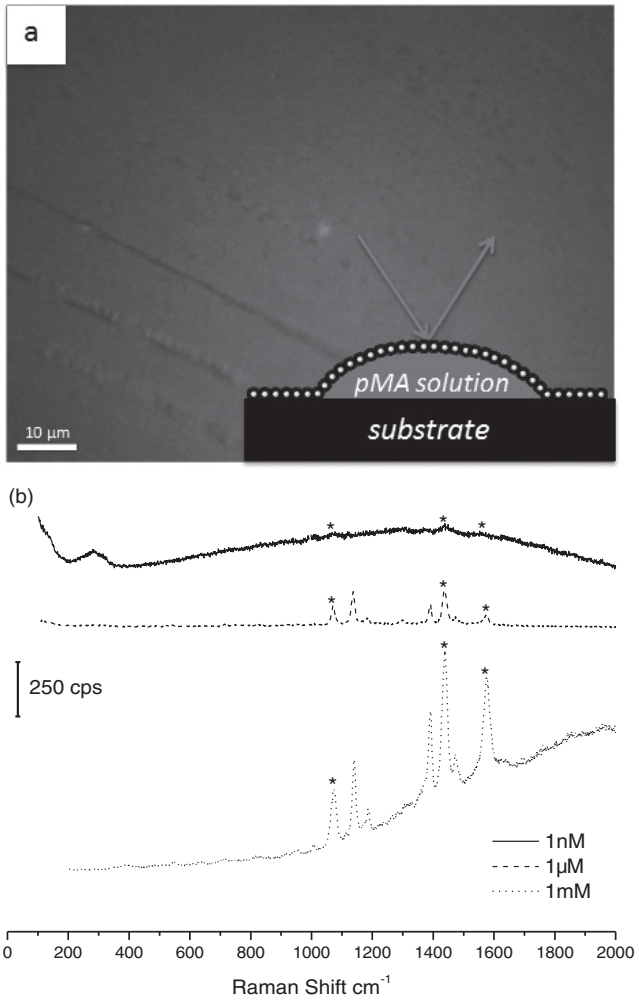

Figure 3. a) Optical image of a gold-nanoparticle sheet self-assembled on top of a *p*MA solution droplet. Inset: sketch of the geometry. b) SERS spectra from in-situ measurements on *p*MA solution droplets of different concentrations covered by gold-nanoparticle sheets. As low as 1 nM, the characteristic Raman peaks of *p*MA can be identified, as indicated by the stars. Excitation wavelength: 633 nm; laser power: 10% (0.47 mW); acquisition time per trace: 10 s. Curves are shifted for clarity.

3. Conclusion

In conclusion, we have demonstrated the in-situ sintering of self-assembled sheets of small ligated gold nanoparticles into larger nanoparticle assemblies with very narrow gaps. This provides a dramatic overall enhancement of Raman scattering, and in particular opportunities for probe molecules to get sufficiently close to the particles for strong chemical enhancement. This approach inherits some of the key advantages of SERS performed with colloidal solutions. At the same time it offers extreme simplicity as well as versatility, thus allowing both for in-situ SERS on droplets of aqueous solutions by coating them with a nanoparticle monolayer, and for the design of novel solid SERS substrates by draping a nanoparticle sheet over a thin freestanding Si_3N_4 window. The very high sensitivity of this SERS chip design was demonstrated with both *p*MA and 2,4-DNT molecules.

4. Experimental Section

Nanoparticle Synthesis: Au nanoparticles were synthesized by reducing Au salt with sodium borohydride in an inverse micelle solution, followed by a digestive ripening process using an excess amount of dodecanethiol ligand to narrow the particle size.[8] TEM analysis of the samples showed average diameters of ≈5.5 nm with size dispersion <10%.

Sample Preparation: *p*-Mercaptoaniline (*p*MA, 97%) and 2,4-dinitrotoluene (2,4-DNT, analytical standard acetonitrile solution) were purchased from Sigma–Aldrich and used as received. Ultrapure deionized water (Nanopure system) was used throughout the experiments. Silicon substrates (3 mm × 4 mm) coated with 100 nm silicon nitride were used. At two spots near the center of each substrate, the silicon was etched away from the back side to create square, TEM-transparent silicon nitride "window" areas ≈60 μm along the side. The substrates were spin-washed several times with toluene, methanol, acetone, and ultrapure water. The self-assembled nanoparticle sheets were prepared by following the procedure published in our previous work.[7a,9] Briefly, the substrate was placed on a clean glass slide or a piece of Teflon tape. A pure water droplet (8 μL) was deposited, and then nanoparticle solution (20 μL) was applied on top of the water droplet. Due to the low surface tension of toluene, the nanoparticle solution expanded and quickly covered the water droplet. After the toluene evaporated in several minutes, a monolayer of nanoparticles was left at the water/air interface and dried onto the substrate under ambient conditions. Due to the decrease in surface area by almost 50%, some folds (corresponding to triple layers of nanoparticles) developed during the drying process. For use as a solid SERS substrate, *p*MA solution droplets (8 μL) of different concentrations

 © 2011 Wiley-VCH Verlag GmbH & Co. KGaA, Weinheim

were deposited on top of the dried nanoparticle layer and allowed to evaporate under ambient conditions. For the in-situ measurements in Figure 3, pure water droplets (8 μL) were replaced by *p*MA solution droplets (8 μL) of different concentrations and SERS measurements were taken before the droplets had dried.

Optical Microscopy and TEM: TEM imaging was conducted using a Tecnai F30 microscope with accelerating voltage at 300 kV. Optical micrographs were taken with an Olympus BH-2 microscope.

SERS Measurements: SERS spectra were recorded on a Renishaw inVisa Raman microscope using a 50× objective (NA = 0.75). For the in-situ experiments on droplets shown in Figure 3, a long-working-distance 50× objective with NA = 0.5 was used. A He–Ne laser (633 nm) was used for the excitations. The laser beam size focused on the samples was 2 μm in diameter with a laser power of 4.7 mW at 100%.

Supporting Information

Supporting Information is available from the Wiley Online Library or from the author.

Acknowledgements

We thank Dr. David Gosztola at the Center for Nanoscale Materials, Argonne National Laboratory, for help with the SERS measurements. This work was supported by the NSF through DMR-0907075. The Chicago MRSEC, supported by the NSF under DMR-0820054, is gratefully acknowledged for access to its shared experimental facilities. The work at Argonne was supported by the U.S. Department of Energy (DOE), BES-Materials Sciences, under Contract #DE-AC02-06CH11357, and by the DOE Center for Nanoscale Materials.

[1] a) M. Fleischm, P. J. Hendra, A. J. McQuilla, *Chem. Phys. Lett.* **1974**, *26*, 163; b) M. G. Albrecht, J. A. Creighton, *J. Am. Chem. Soc.* **1977**, *99*, 5215; c) D. L. Jeanmaire, R. P. Vanduyne, *J. Electroanal. Chem.* **1977**, *84*, 1; d) C. L. Haynes, A. D. McFarland, R. P. Van Duyne, *Anal. Chem.* **2005**, *77*, 338A.

[2] a) L. Gunnarsson, E. J. Bjerneld, H. Xu, S. Petronis, B. Kasemo, M. Kall, *Appl. Phys. Lett.* **2001**, *78*, 802; b) H. H. Wang, C. Y. Liu, S. B. Wu, N. W. Liu, C. Y. Peng, T. H. Chan, C. F. Hsu, J. K. Wang, Y. L. Wang, *Adv. Mater.* **2006**, *18*, 491; c) J. T. Bahns, Q. T. Guo, J. M. Montgomery, S. K. Gray, H. M. Jaeger, L. H. Chen, *J. Phys. Chem. C* **2009**, *113*, 11190; d) D. P. Fromm, A. Sundaramurthy, A. Kinkhabwala, P. J. Schuck, G. S. Kino, W. E. Moerner, *J. Chem. Phys.* **2006**, *124*, 061101; e) B. Yan, A. Thubagere, W. R. Premasiri, L. D. Ziegler, L. Dal Negro, B. M. Reinhard, *ACS Nano* **2009**, *3*, 1190; f) J. F. Li, Y. F. Huang, Y. Ding, Z. L. Yang, S. B. Li, X. S. Zhou, F. R. Fan, W. Zhang, Z. Y. Zhou, D. Y. Wu, B. Ren, Z. L. Wang, Z. Q. Tian, *Nature* **2010**, *464*, 392.

[3] a) K. Kneipp, Y. Wang, H. Kneipp, L. T. Perelman, I. Itzkan, R. Dasari, M. S. Feld, *Phys. Rev. Lett.* **1997**, *78*, 1667; b) S. M. Nie, S. R. Emery, *Science* **1997**, *275*, 1102; c) K. Kneipp, H. Kneipp, R. Manoharan, E. B. Hanlon, I. Itzkan, R. R. Dasari, M. S. Feld, *Appl. Spectrosc.* **1998**, *52*, 1493.

[4] H. X. Xu, J. Aizpurua, M. Kall, P. Apell, *Phys. Rev. E* **2000**, *62*, 4318.

[5] a) N. R. Jana, T. Pal, *Adv. Mater.* **2007**, *19*, 1761; b) Y. Yang, J. L. Shi, T. Tanaka, M. Nogami, *Langmuir* **2007**, *23*, 12042; c) H. Ko, S. Singamaneni, V. V. Tsukruk, *Small* **2008**, *4*, 1576.

[6] a) A. Wei, B. Kim, B. Sadtler, S. L. Tripp, *ChemPhysChem* **2001**, *2*, 743; b) K. W. Kho, Z. X. Shen, H. C. Zeng, K. C. Soo, M. Olivo, *Anal. Chem.* **2005**, *77*, 7462; c) H. Wang, C. S. Levin, N. J. Halas, *J. Am. Chem. Soc.* **2005**, *127*, 14992.

[7] a) J. B. He, P. Kanjanaboos, N. L. Frazer, A. Weis, X. M. Lin, H. M. Jaeger, *Small* **2010**, *6*, 1449; b) J. He, X.-M. Lin, H. Chan, L. Vuković, P. Král, H. M. Jaeger, *Nano Lett.* **2011**, *11*, 2430.

[8] X. M. Lin, H. M. Jaeger, C. M. Sorensen, K. J. Klabunde, *J. Phys. Chem. B* **2001**, *105*, 3353.

[9] K. E. Mueggenburg, X. M. Lin, R. H. Goldsmith, H. M. Jaeger, *Nat. Mater.* **2007**, *6*, 656.

[10] a) W. Hill, B. Wehling, *J. Phys. Chem.* **1993**, *97*, 9451; b) M. Osawa, N. Matsuda, K. Yoshii, I. Uchida, *J. Phys. Chem.* **1994**, *98*, 12702.

[11] K. A. Willets, R. P. Van Duyne, *Annu. Rev. Phys. Chem.* **2007**, *58*, 267.

[12] Y. Y. Wang, Z. H. Ni, Z. X. Shen, H. M. Wang, Y. H. Wu, *Appl. Phys. Lett.* **2008**, *92*, 043121.

[13] B. Pettinger, U. Wenning, H. Wetzel, *Chem. Phys. Lett.* **1979**, *67*, 192.

[14] G. K. Liu, J. Hu, P. C. Zheng, G. L. Shen, J. H. Jiang, R. Q. Yu, Y. Cui, B. Ren, *J. Phys. Chem. C* **2008**, *112*, 6499.

[15] D. Y. Wu, X. M. Liu, Y. F. Huang, B. Ren, X. Xu, Z. Q. Tian, *J. Phys. Chem. C* **2009**, *113*, 18212.

[16] a) A. Gopinath, S. V. Boriskina, W. R. Premasiri, L. Ziegler, B. M. Reinhard, L. Dal Negro, *Nano Lett.* **2009**, *9*, 3922; b) S. J. Tan, M. J. Campolongo, D. Luo, W. Cheng, *Nat. Nanotechnol.* **2011**, *6*, 268.

[17] S. C. Yang, X. W. Wan, Y. T. Ji, L. Q. Wang, X. P. Song, B. J. Ding, Z. M. Yang, *CrystEngComm* **2010**, *12*, 3291.

[18] a) W. Y. Li, P. H. C. Camargo, X. M. Lu, Y. N. Xia, *Nano Lett.* **2009**, *9*, 485; b) D. K. Lim, K. S. Jeon, H. M. Kim, J. M. Nam, Y. D. Suh, *Nat. Mater.* **2010**, *9*, 60.

[19] a) J. M. Sylvia, J. A. Janni, J. D. Klein, K M. Spencer, *Anal. Chem.* **2000**, *72*, 5834; b) A. Tao, F. Kim, C. Hess, J. Goldberger, R. R. He, Y. G. Sun, Y. N. Xia, P. D. Yang, *Nano Lett.* **2003**, *3*, 1229.

Received: July 29, 2011
Revised: August 22, 2011
Published online: October 21, 2011

 © 2011 Wiley-VCH Verlag GmbH & Co. KGaA, Weinheim

Copyright WILEY-VCH Verlag GmbH & Co. KGaA, 69469 Weinheim, Germany, 2011.

NANO MICRO small

Supporting Information

for *Small*, DOI: 10.1002/smll.201101534

In-Situ Partial Sintering of Gold-Nanoparticle Sheets for SERS Applications

*Jinbo He , Xiao-Min Lin , Ralu Divan , and Heinrich M. Jaeger**

Supplement

In-situ Partial Sintering of Gold Nanoparticle Sheets for SERS Applications

Jinbo He,[1] Xiao-Min Lin,[2] Ralu Divan,[2] Heinrich M. Jaeger[1]

[1] James Franck Institute, University of Chicago, Chicago, IL 60637

[2] Center for Nanoscale Materials, Argonne National Laboratory, Argonne, IL 60439

jinboh@uchicago.edu; xmlin@anl.gov; divan@anl.gov; h-jaeger@uchicago.edu

CORRESPONDING AUTHOR: Heinrich M. Jaeger, h-jaeger@uchicago.edu

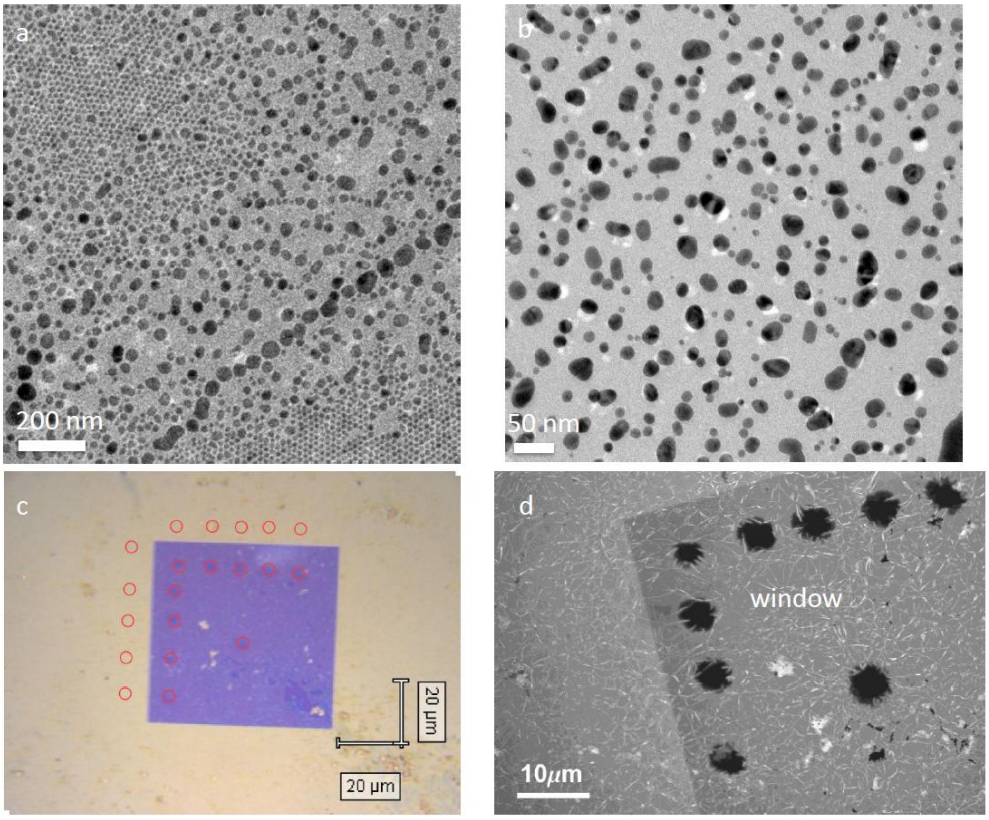

Figure S1. (a-b) TEM images taken inside a spot on the Si3N4 window area that was exposed to 10% laser power for 10s. Results for two different samples are shown in panels (a) and (b), demonstrating similar sintering behavior with similar particle

organization and size distribution. (c) Optical image of a sample after exposure to 10% laser power, showing areas both on the window and outside it. Inside the window, the beam damage is clearly observable. The red circles indicate the locations targeted by the beam outside of window. (d) SEM image of the same sample as in (c). The beam damage to the nanoparticle layer inside the window is immediately obvious. However, outside of window area even at 10% laser power, no damage to the gold nanoparticle sheet is seen by SEM (compare for the location of the red circles in (c)).

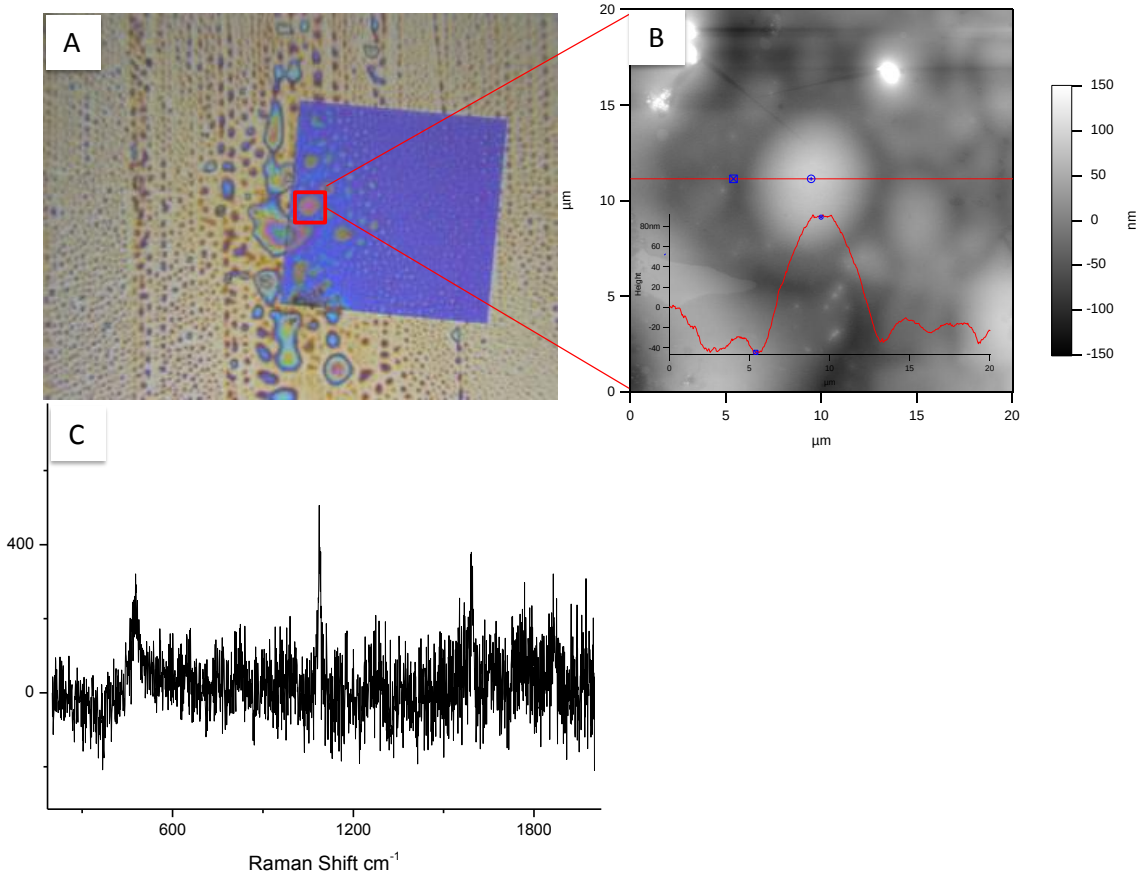

Figure S2. (a) Optical image of *p*MA dried on a clean Si_3N_4/Si substrate. The red square indicates the spot exposed to laser beam. (b) AFM image of the same spot exposed in (a). The horizontal red line indicates the location of the height profile across the exposed area. (c) The Raman spectrum of pure *p*MA on the Si_3N_4 window area, using 10% laser power at 633 nm. Acquisition time was 10s.

In order to calculate the empirical enhancement factor, the Raman spectrum from pure *p*MA on the Si_3N_4 window was taken as a reference. As shown in Figure S1a, 8 μl Ethanol solution (10 mM) of *p*MA was allowed to dry on a clean substrate. The SERS spectrum shown in Figure S1c was recorded on a Renishaw inVisa Raman microscope using a 50x objective (NA= 0.75). A He-Ni laser (633 nm) was used for the excitations. The laser beam size focused on the samples was 2 μm in diameter. 10% laser power (0.47 mW) was used with an acquisition time of 10s. The exact exposed spot in Figure S1a was imaged by AFM to extract the thickness of the sample as shown in Figure S1b. The equation for the enhancement factor is $EF = (I_{SERS}/N_{SERS})/(I_{RS}/N_{RS})$,

where I_{SERS} and I_{RS} are the SERS intensity and normal Raman intensity, respectively, normalized for acquisition time and laser power. N_{SERS} and N_{RS} are the number of molecules probed in the SERS and Raman measurements. The Raman shift at 1080 cm^{-1}, belonging to the *a1* symmetry that is mostly affected by physical enhancement, is chosen to be the peak for comparison. For the normal Raman spectrum of *p*MA, using a bulk density of 1.18 g/cm^3, I_{RS}/N_{RS} gives a value of $3.6x10^{-8}$ count/(molecule•s•mW). For the SERS spectrum at 1pM, assuming a homogeneous distribution of *p*MA across the 3mm × 4mm substrate, a I_{SERS}/N_{SERS} value of 139 count/(molecule•s•mW) is found. This results in an enhancement factor $EF \sim 4x10^9$, which is a conservatively estimated value due to the over-estimation of the surface area.